

Structure and Properties of Burnished and Nitrided AISI D2 Tool Steel

Daniel TOBOLA¹, Witold BROSTOW^{2*}, Kazimierz CZECHOWSKI¹, Piotr RUSEK¹,
Iwona WRONSKA¹

¹Institute of Advanced Manufacturing Technology (IAMT), Wroclawska 37a, 30-011 Cracow, Poland

²Laboratory of Advanced Polymers & Optimized Materials (LAPOM), Department of Materials Science and Engineering, Department of Physics and Center for Advanced Research and Technology (CART), University of North Texas, 3940 North Elm Street, Denton, TX 76207, USA

crossref <http://dx.doi.org/10.5755/j01.ms.21.4.7224>

Received 01 June 2014; accepted 25 December 2014

D2 belongs to traditional steels, frequently used in metalworking industry. Shot peening and nitriding are known to improve the wear resistance of D2. In this work we focus on processes of slide burnishing and industrial low temperature gas nitriding. The D2 steel specimens were first subjected to heat treatments (HT) prescribed by the manufacturer, turning (T), then burnishing (B) and nitriding (N). The reason for turning was achieving appropriate surface roughness. Deformation induced in slide burnishing can be better controlled then in shot peening because of deterministic nature of this process. Four different paths to prepare surfaces were employed: HT + T, HT + T + B, HT + T + N, HT + T + B + N. D2 steel is very sensitive to the final finishing, wear rates vary up to 300 %. Two of our procedures (HT + T + N and HT + T + B + N) are much superior to the others. Moreover, in the HT + T + N case, apparently the surface fatigue scaling off takes place.

Keywords: steel slide diamond burnishing, steel nitriding, tool steel, steel wear.

1. INTRODUCTION

Burnishing of metalworking tools can lead to wear resistance improvement as well as longevity increase. Usually metalworking tools comprise entire fixtures and operate in high productivity production lines. Needless to say, long down-time means low output, high cost and loss of competitiveness of the plant. We believe that improvement of manufacturing technologies is more economical than highly praised development of new materials.

Among the popular traditional tool materials – Sverker 21 (AISI D2) is recognized as inexpensive and good for many industrial applications. Numerous publications deal with this high chromium steel and with some of its improvements such as addition of molybdenum or titanium with parallel carbon and chromium reduction [1], as well as treatment improvements (including nitriding) [2–6]. Laboratory testing of various kinds have been performed – but to our knowledge no testing in service; necessarily, the latter is more time consuming and more difficult to perform. Hashami and co-workers [7] have reported some benefits of shot peening. Berkowski and Borowski [8] reported some advantages of nitriding. We have worked on steel property improvement primarily by slide diamond burnishing [9, 10]. On the basis of the literature and our own results, in the present work we have focused on various combinations of heat treatment (HT), turning (T), burnishing (B) and nitriding (N). The following sequences were followed: HT + T, HT + T + B, HT + T + N, HT + T + B + N.

2. EXPERIMENTAL

Specimens of ledeburitic chromium-alloyed tool steel AISI D2 (known under the trade name Sverker 21), were obtained by a conventional metallurgical process. The respective chemical composition is shown in Table 1. The specimens were machined and subjected to a heat treatment (austenizing temperature 1035 ÷ 1040 °C, soaked 4 min 40 s; double tempering for 2 h at 530 °C and 520 °C) aimed at reaching the Rockwell Hardness of ≈ 60 HRC.

Table 1. Chemical composition of the studied tool steel in wt. %

C	Si	Mn	Cr	Mo	V
1.55	0.3	0.4	11.8	0.8	0.8

After heat treatment, longitudinal turning of the bar probe with a tool insert holder was performed first. The following turning conditions were maintained: turning speed $v_c = 100$ m/min, feed $f = 0.17$ mm/rev, cutting depth $a_p = 0.1$ mm. Polycrystalline cubic boron nitride (PCBN) cutting inserts made by Mitsubishi under the trade name NP-SNGA 120412GS2 MB730 were used. The surface roughness R_a is defined as the arithmetic average height of roughness-component irregularities (peak heights and valleys) from the mean line, measured within the sampling length. Our R_a values are averages of 6 measurements. Before burnishing, we obtained the R_a values between 0.72 and 0.82 μm . Turning improves the surface geometry, thus affecting the roughness.

Slide diamond burnishing process of our steel in the quenched state was carried out using diamond tools (Fig. 1) designed by us and currently produced by the Institute of Advanced Manufacturing Technology (IAMT), with the tips made of diamond composites with ceramic

* Corresponding author. Tel.: +1-940-565-4358; fax: +1-940-565-4824.
E-mail address: konradb09@gmail.com (W. Brostow)

bonding phase, namely Ti_3SiC_2 [11, 12] and the shape of spherical caps with the radius $R = 1.5$ mm.



Fig. 1. Diamond burnisher with tool holder and working parts (spherical cups)

Surface treatments involving both turning and burnishing were carried out on shaft end faces, using fixing system for tools (lathe and burnisher tool) perpendicular to the face; see Fig. 2.

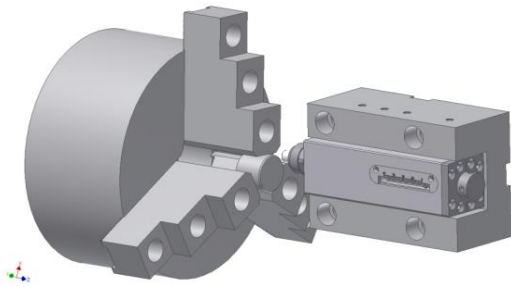


Fig. 2. The fixing of diamond slide burnisher tool

After turning or turning + burnishing process, selected surfaces were immediately nitrided by gas nitriding, under typical conditions defined in Table 2. This technology has been prescribed as one of the operations in the design and manufacturing of tools, dies, etc.

Table 2. Nitriding process parameters

Stage	Process temperature, °C	Time, h
First stage	520	5
Second stage	535	20

The surface roughness parameters were measured with the Hommel Tester T1000 profilometer and also with laboratory profilometer TOPO 01 developed at IAMT.

Surface layer microstructures and nitrogen distributions in HT+T+N and HT+T+B+N specimens were determined using a JEOL JSM 6460 V digital scanning electron microscope equipped with an energy dispersive X-ray spectrometer (EDS).

Transverse metallographic specimens were examined after earlier preparation on metallographic grinding - polisher RotoPol 21. Mounting of samples was done in thermosetting resins in a CitoPress device. The nitrogen content at a given distance from the specimen surface is a mean value for the scanned microspheres shown in Fig. 3. In general, such microanalytical method is not recommended for the quantitative analysis of elements with low atomic numbers, i.e. carbon, nitrogen or boron. However, we are using it for comparative purposes.

Vickers microhardness $h_{Vickers}$ was determined using a FM 7 tester from Future Tech. Corp., Japan. Microindentations were made using a 200 g load.

The abrasive wear resistance was evaluated by using the ball-on-disc method; see for instance [13]. A UMT-

2MT universal mechanical tester made by CETR, Campbell, CA, USA was used.

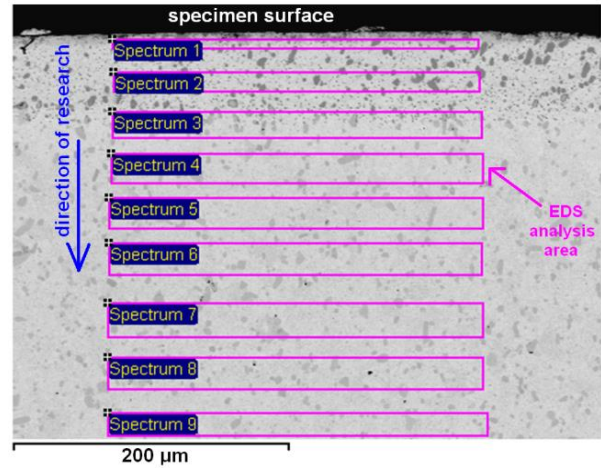


Fig. 3. Image of turned burnished and nitrided specimens with marked EDS analysis areas

The ball and disc samples were washed in ethyl alcohol and dried before the measurement. The loading mechanism applies a controlled load F_n to the ball holder while the friction force is measured continuously during the test using an extensometer. For each test, a new ball was used or the ball was rotated so that a new surface was in contact with the disc.

The size of the disc-shaped samples was approximately 30 mm diameter and 20 mm in height, with the surfaces flatness and parallelism within 0.02 mm. The following test conditions were applied: Al_2O_3 ball diameter 3.2 mm, applied load 6.0 N, sliding speed 0.1 m/s, diameter of the sliding circle 8.0 mm, sliding distance 2000 m, calculated duration of the test $2 \cdot 10^4$ s. The tests were carried out without a lubricant at room temperature. Dynamic friction μ was calculated using the standard

formula: $\mu = \frac{F_f}{F_n}$ where F_f is the measured friction force

while F_n is the applied normal force. After completing the tests following the ISO 20808:2004 E standard, the cross-sectional profile of each wear track was measured at four places, at intervals of 90° , using a contact stylus profilometer TOPO 01. Then the average cross-sectional area of the wear track was calculated. The volume of material removed was calculated as a product of cross-sectional area of the wear track and their circumference. Specific wear rate W_s was calculated by the standard formula: $W_s = \frac{V}{F_n \cdot L}$ where V is the volume of removed material and L is the sliding distance.

As expected, the roughness of the tested surface before wear testing was dependent on the type of surface treatment used; see Table 3.

Table 3. Type of surface treatment and resulting roughness

Surface treatment	Sample code	Mean roughness Ra , μm
HT+T	S.1	0.8
HT+T+B	S.2	0.24
HT+T+N	S.3	0.72
HT+T+B+N	S.4	0.23

3. RESULTS AND DISCUSSION

In Fig. 4 we display a typical microstructure of quenched and tempered AISI D2 steel; we see carbide particles in a fine tempered martensite structure.

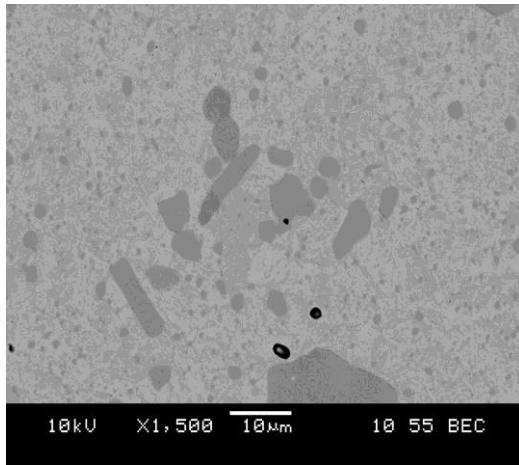


Fig. 4. SEM micrographs of AISI D2 tool steel structure after quenching and tempering

The results of surface roughness measurements and the resulting K_{Ra} index (the ratio of the roughness after turning to burnishing) after the surface treatment processes are presented in Table 4; parameters listed are determined according to ISO 4287: L_t – 4.8 mm (transverse length); R_a – arithmetical mean deviation of the assessed profile; R_z – the average maximum profile height of the ten largest peak-to-valley separations in the evaluation area; R_p – the maximum profile peak height, i.e. the distance from the mean line/surface to the highest point in the evaluation length/area; R_t – total height of the profile; $Rmr(c)$ – relative material ratio of the profile. The ratio is determined by the intersecting line which separates the protruding peaks from the surface profile. The term bearing area curve (BAC) is also used for the ratio. Lowering the line into the surface results in increasing percentages of the length of the line intersecting protruding peaks. Here results in the last column of the Table pertain to $c = 50\%$.

We see that slide burnishing favourably affects the surface geometric structure (SGS) of the tool steel. The optimised burnishing parameters ($F = 180$ N, $f = 0.02$ mm/rev) substantially affect the surface characteristics and thus K_{Ra} . The respective parameters are defined at the bottom of Table 4. It is seen from the roughness profiles in Fig. 5 that the height of the profile decreases after burnishing. There is reduction, by more

than a factor of two, of the parameter $c\%$, namely R_t for $Rmr'(c) = 50\%$; we see also a concurrent increase in the material ratio (Fig. 6), what substantially increases the area of tool/workpiece contact.

Fig. 7 shows the cross-sectional microstructure of our D2 steel subjected to various surface treatment processes. The presence of the compound layer can be clearly observed. In the case of the turning+burnishing+nitriding series (Fig. 7 b), the thickness of the nitrided zone is almost double as compared to turned and nitrided only.

We have also determined the Vickers microhardness $h_{Vickers}$, a quantity we have used before and we find convenient to characterize also other types of materials and coatings [14]. In the case of nitrided surfaces of D2 steel, we observe a significant increase of the microhardness (Fig. 8). That increase, in particular down to a 80 μ m depth below the surface, is in range $4 \div 44\%$ for burnished surfaces – as compared to surfaces nitride only.

Nitrogen content at a given distance from the sample surface is the average value for an area of about $260 \times 8 \mu$ m. A method of data collection was shown in Fig. 3. The results are summarized in Fig. 9.

There are substantial differences in nitrogen content between cross-sections in T+N and T+B+N samples. At $\approx 100 \mu$ m below the surface, the differences exceed 150%. These observations correlate with the microstructure, in which a clear difference is observed between the thickness and uniformity of the nitriding of the tool steel. A similar trend is evident also in the microhardness profiles (Fig. 8).

The dynamic friction μ , is shown in Fig. 10 as a function of the testing time. After turning, the friction increases with sliding time up to about 60 min.; at that time μ reaches a practically constant value of about 0.9. A similar trend can be observed after burnishing, but then the friction settles at a lower value of approximately 0.8. A different trend is observed after turning and nitriding. Two degradation stages occur after about 2 h and 4.5 h. They seem to correspond to surface fatigue scaling off. A similar phenomenon has been observed by Staia et al. [15]. Sequential processing: turning + burnishing + nitriding results in the lowest value of the dynamic friction of approximately 0.75.

Wear rates calculated as explained above are displayed in Fig. 11. We find significant differences between the results for different treatment sequences. Turning alone does not improve much wear resistance of our D2 specimens. Further surface treatments like nitriding or/and burnishing provide better results. Burnishing alone can increase by almost 40% the wear resistance of the turned specimens.

Table 4. Mean values (averages from 6 measurements) of surface geometric characteristics parameters

Sample Code	Burnishing Force, N	Feed, mm/rev	SGS parameters after turning					SGS parameters after burnishing					K_{Ra}
			R_a' , μ m	R_z' , μ m	R_p' , μ m	R_t' , μ m	$c', \% Rt'$ for $Rmr'(c)=50\%$	R_a , μ m	R_z , μ m	R_p , μ m	R_t , μ m	$c, \% Rt$ for $Rmr(c)=50\%$	
S.1	Turning		0.79	3.31	1.91	3.49	59.9	–	–	–	–	–	–
S.2	180	0.02	0.82	3.51	2.21	4.02	59.7	0.24	1.70	0.90	2.11	39.8	3.38
S.3	Turning		0.72	3.14	2.01	3.52	64.8	–	–	–	–	–	–
S.4	180	0.02	0.75	3.33	2.10	3.62	64.9	0.23	1.56	1.24	2.21	54.8	3.22

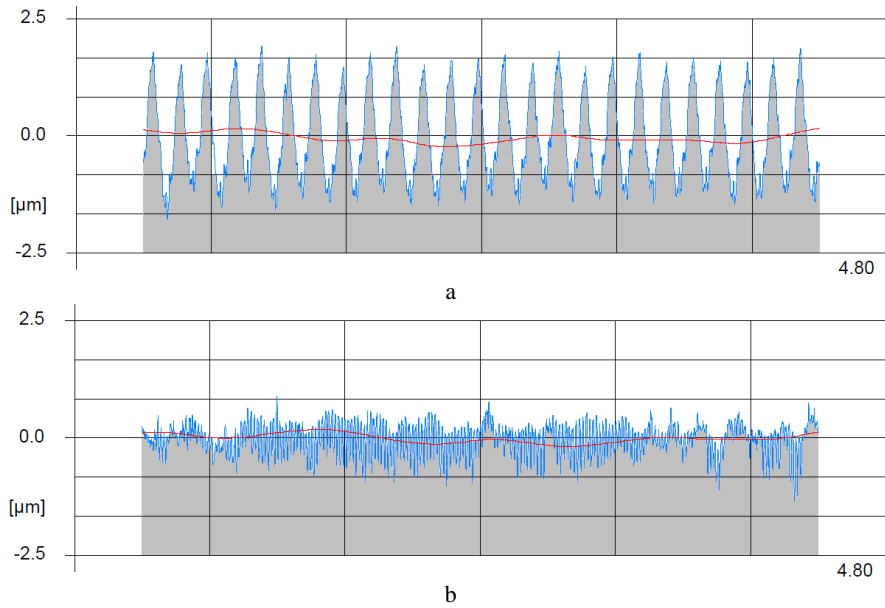


Fig. 5. Examples of the profilographs for the specimens surface after: a – turning; b – turning + burnishing.

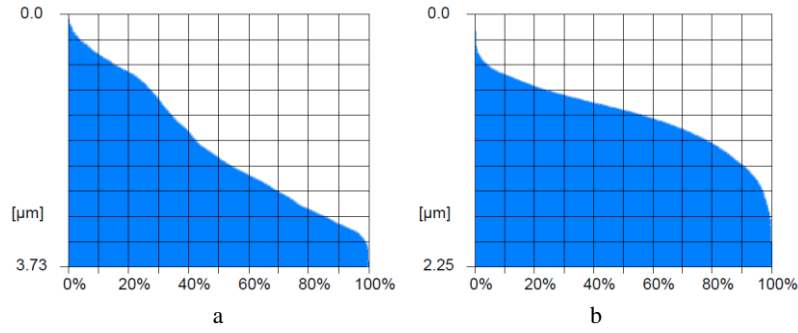


Fig. 6. Examples of the material ratio of the profile for the specimens surface after: a – turning; b – turning + burnishing

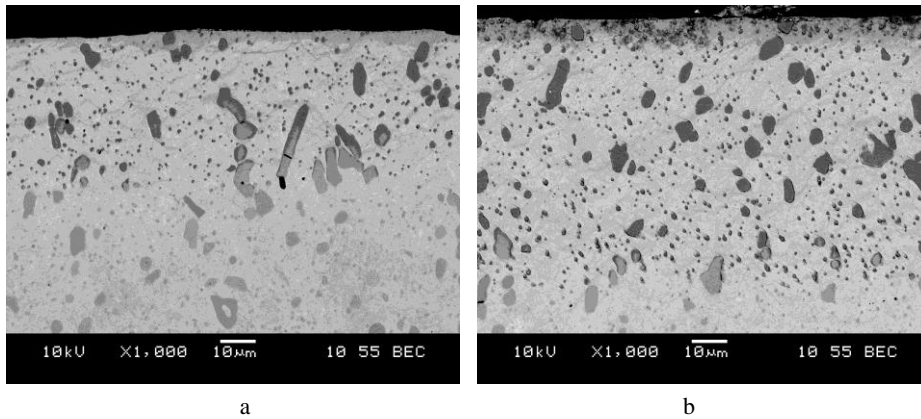


Fig. 7. Cross-sectional SEM micrographs of the surface layer: a – turning+ nitriding; b – turning+ burnishing+ nitriding

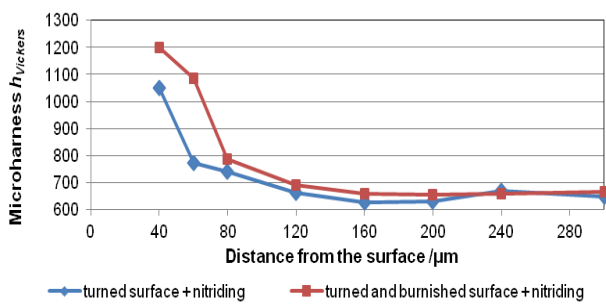


Fig. 8. Microhardness of D2 specimens after turning, slide diamond burnishing and nitriding

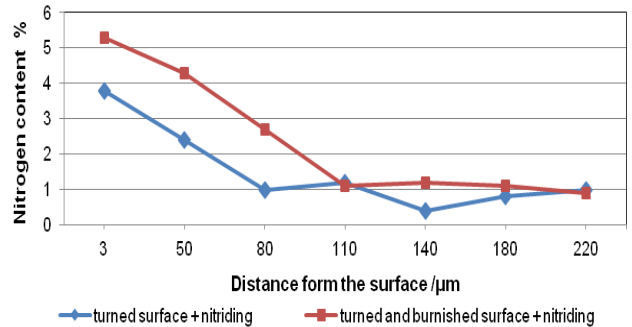


Fig. 9. Distributions of nitrogen content of D2 specimens after turning, slide diamond burnishing and nitriding

Nitriding can have a very strong influence, 150 % improvement. On the other hand, very high hardness of the upper surface layer favours formation of microfractures; the consequences are seen in Fig. 10. The best results are seen for T + B + N specimens (green line in Fig. 10): no scale offs, low value of friction and more than 200 % higher wear resistance in tribometry. Those results confirm the expectation that the synergy effect exists in multistage treatments, as contrasted with single nitriding or burnishing.

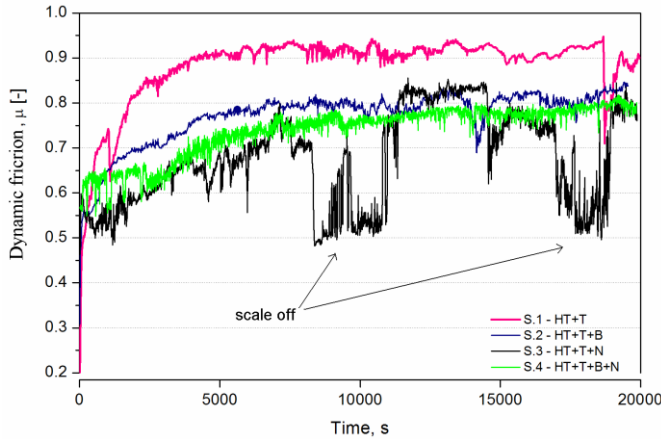


Fig. 10. Changes in the dynamic friction μ for D2 tool steel after various surface treatments

4. CONCLUDING REMARKS AND A SURVEY OF RESULTS

Quite understandably, much research effort is expended in providing steels with a protection from corrosion [16]. The issue of wear concerns only applications when moving parts are involved [17]. However, in those cases we have a similar situation as with corrosion: an otherwise usable part has to be replaced by a new one—while later on the replacement will have to be repeated periodically. Aydin, Bayram and Topçu [18] studied effects of nitriding on AISI 430 ferritic stainless steel. They have performed nitriding in gas mixtures and also in salt baths. Clear effects of the nitriding medium and also of the temperature on dynamic friction have been reported. Important conclusions from our work can be summarized as follows:

1. Diamond slide burnishing before gas nitriding improves wear abrasive resistance of D2 tool steel by nearly 20 %;

2. Burnishing alone increases the abrasive wear resistance by 37 % in comparison with heat treated and turned specimens;
3. Although HT + T + N samples have a good wear resistance in ball-on-disc testing (only 18 % below the best HT + T + B + N combination), two sudden falls of μ which correspond to scaling off upper layers of the surface (debris formation) occur. Needless to say, peeling the surface is unacceptable for many engineering applications since under dynamic loads a sudden fracture of manufactured elements becomes possible;
4. Comparison with the results of Berkowski and Borowski [8] shows that even less advantageous conditions (higher nitriding temperatures) lead to property improvement in diamond slide burnishing followed by ordinary gas nitriding process.

Acknowledgments

We thank the Materials Engineering and Sintering Centre team of IAMT for their support.

REFERENCES

1. **Viale, D., Béguinot, J., Chenou, F., Baron, G.** Optimizing Microstructure for High Toughness Cold-Work Tool Steels. *Proceedings of the 6th International Tooling Conference* 2002: pp. 299–318.
2. **Čerňan, J., Rodziňák, D., Komolík, M., Hvizdoš, P., Semrád, K.** Tribological Properties of Sintered Steel Following Plasma Nitriding *Powder Metallurgy Progress* 1 (12) 2012: pp. 34–42.
3. **Karamiş, M.B., Gerçekcioğlu, E.** Wear Behaviour of Plasma Nitrided Steels at Ambient and Elevated Temperatures *Wear* 243 2000: pp. 76–84.
4. **Pessin, M.A., Tier, M.D., Strohaecker, T.R., Bloyce, A., Sun, Y., Bell, T.** The Effects of Plasma Nitriding Process Parameters on The Wear Characteristics of AISI M2 Tool Steel *Tribology Letters* 8 2000: pp. 223–228. <http://dx.doi.org/10.1023/A:1019199604963>
5. **Suchánek, J., Kukulík, V.** Influence of Heat and Thermochemical Treatment on Abrasion Resistance of Structural and Tool Steels *Wear* 267 2009: pp. 2100–2108.
6. **Jurci, P.** Saturation of The Cr-V Ledeburitic Steel with Nitrogen *Kovove Materialy – Metallic Materials* 48 2010: pp. 217–226.

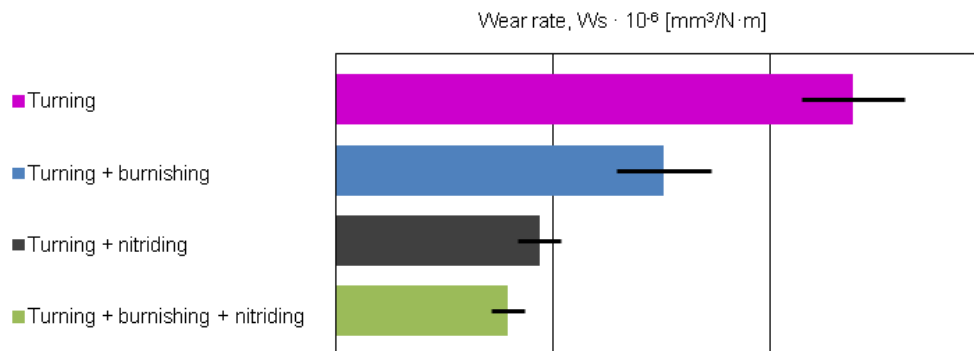


Fig. 11. Wear rates for D2 tool steels after different surface treatments (load: 6.0 N, speed: 0.1 m/s, sliding distance: 2.0 km)

7. **Hashami, B., Yazdi, M.R., Azar, V.** The Wear and Corrosion Resistance of Shot Peened – Nitrided 316L Austenitic Stainless Steel *Materials and Design* 32 2011: pp. 3287–3292.
<http://dx.doi.org/10.1016/j.matdes.2011.02.037>
8. **Berkowski, L., Borowski, J.** The Influence of Structure on The Results of The Nitriding of Ledeburitic Chromium Steels, Part VIII, Investigation of Utilization Properties of Tool Materials *Obróbka Plastyczna Metali* XX (4) 2009: pp. 13–16 (in Polish).
9. **Bednarski, P., Bialo, D., Brostow, W., Czechowski, K., Polowski, W., Rusek P., Toboła, D.** Improvement of Tribological Properties of Metal Matrix Composite by Means of Slide Burnishing *Materials Science (Medziagotyra)* 19 2013: pp. 367–372.
10. **Brostow, W., Czechowski, K., Polowski, K., Rusek, P., Toboła, D., Wronska, I.** Slide Diamond Burnishing of Tool Steel with Adhesive Coatings and Diffusion Layers *Materials Research Innovations* 4 (17) 2013: pp. 269–277.
11. **Jaworska, L., Szutkowska, M., Morgiel, J., Stobierski, L., Lis, J.** Ti₃SiC₂ as a Bonding Phase in Diamond Composites. *Journal of Materials Science Letters* 20 2001: pp. 1783–1786.
<http://dx.doi.org/10.1023/A:1012535100330>
12. **Jaworska, L., Stobierski, L., Twardowska, A., Królicka, D.** Preparation of Materials Based on Ti–Si–C Systems using High Temperature–High Pressure Method. *Journal of Materials Processing Technology* 162–163 2005: pp. 184–189.
13. **Brostow, W., Deborde, J.L., Jaklewicz, M., Olszynski, P.** Tribology with Emphasis on Polymers: Friction, Scratch Resistance and Wear *Journal of Materials Education* 25 2003: pp. 119–132.
14. **Brostow, W., Kovacevic, V., Vrsaljko, D., Whitworth, J.** Tribology of Polymers and Polymer-Based Composites *Journal of Materials Education* 32 2010: pp. 273–290.
15. **Brostow, W., Chonkaew, W., Rapoport, L., Soifer, Y., Verdyan, A.** Grooves in Scratch Testing *Journal of Materials Research* 22 2007: pp. 2483–2487.
16. **Brostow, W., Datashvili, T., Geodakyan, J.** Tribological Properties of EPDM + PP + Thermal Shock-Resistant Ceramic Composites *Polymer International* 61 2012: pp. 1362.
<http://dx.doi.org/10.1002/pi.4282>
17. **Staia, M.H., Pérez-Delgado, Y., Sanchez, C., Castro, A., Le Bourhis, E., Puchi-Cabrera, E.S.** Hardness Properties and High-Temperature Wear Behaviour of Nitrided AISI D2 Tool Steel, Prior and After PAPVD Coating *Wear* 267 2009: pp. 1452–1461.
18. **Minkevicius, A., Levinskas, R., Lukosiute, I., Kvikys, A.** Stainless 08X18H10T and Low-Alloyed 15X1M1Φ Steels Protection from Corrosion With Emulsions of Thermostable Amines *Materials Science (Medziagotyra)* 9 2003: pp. 342–346.
19. **Babilius, A., Ambroza, P.** Effect of Temperature and Sliding Speed on The Adhesive Wear *Materials Science (Medziagotyra)* 9 2003: pp. 347–350.
20. **Aydin, H., Bayram, A., Topçu, S.** Friction Characteristics of Nitride Layers on AISI 430 Ferritic Stainless Steel Obtained by Various Nitriding Processes *Materials Science (Medziagotyra)* 19 2013: pp. 19–24.